A novel yeast hybrid modeling framework integrating Boolean and enzyme-constrained networks enables exploration of the interplay between signaling and metabolism

Linnea Österberg[1,2,3], Iván Domenzain [3,4], Julia Münch[1,2], Jens Nielsen[3,4,5], Stefan Hohmann [3], Marija Cvijovic[1,2*]

[1] Department of Mathematical Sciences, University of Gothenburg, Gothenburg, Sweden

[2] Department of Mathematical Sciences, Chalmers University of Technology, Gothenburg, Sweden

[3] Department of Biology and Biological Engineering, Chalmers University of Technology, Gothenburg, Sweden

[4] Novo Nordisk Foundation Center for Biosustainability, Chalmers University of Technology, SE41296 Gothenburg, Sweden

[5] BioInnovation Institute, Ole Maaløes Vej 3, DK2200 Copenhagen, Denmark

*** Correspondence:**

Marija Cvijovic
marija.cvijovic@chalmers.se

Keywords: hybrid model, enzyme constraints, Boolean model, nutrient signaling, metabolism, protein allocation, multiscale model, *Saccharomyces cerevisiae*

Abstract

The interplay between nutrient-induced signaling and metabolism plays an important role in maintaining homeostasis and its malfunction has been implicated in many different human diseases such as obesity, type 2 diabetes, cancer and neurological disorders. Therefore, unravelling the role of nutrients as signaling molecules and metabolites as well as their interconnectivity may provide a deeper understanding of how these conditions occur. Both signalling and metabolism have been extensively studied using various systems biology approaches. However, they are mainly studied individually and in addition current models lack both the complexity of the dynamics and the effects of the crosstalk in the signaling system. To gain a better understanding of the interconnectivity between nutrient signaling and metabolism, we developed a hybrid model, combining Boolean model, describing the signalling layer and the enzyme constraint model accounting for metabolism using a regulatory network as a link. The model was capable of reproducing the regulatory effects that are associated with the Crabtree effect and glucose repression. We show that using this methodology one can investigat intrinsically different systems, such as signaling and metabolism, in the same model and gain insight into how the interplay between them can have non-trivial effects by showing a connection between Snf1 signaling and chronological lifespan by the regulation of NDE and NDI usage in respiring conditions. In addition, the model showed that during fermentation,

enzyme utilization is the more important factor governing the protein allocation, while in low glucose conditions robustness and control is prioritized.

Author summary

Elucidating the complex relationship between nutrient-induced signaling and metabolism represents a key in understanding the onset of many different human diseases like obesity, type 3 diabetes, cancer and many neurological disorders. In this work we proposed a hybrid modeling approach, combining Boolean representation of singaling pathways, like Snf11, TORC1 and PKA with the enzyme constrained model of metabolism linking them via the regulatory network. This allowed us to improve individual model predictions and elucidate how single components in the dynamic signaling layer affect the steady-state metabolism. The model has been tested under respiration and fermentation, reveling novel connections and further reproducing the regulatory effects that are associated with the Crabtree effect and glucose repression. Finally, we show a connection between Snf1 signaling and chronological lifespan by the regulation of NDE and NDI usage in respiring conditions.

Introduction

Biological systems are of complex nature comprising numerous dynamical processes and networks on different functional, spatial and temporal levels, while being highly interconnected (Walpole et al., 2013). The field of systems biology faces the great challenge of elucidating how these interconnected systems work both separately and together to prime organisms for survival. One of such phenomena is the cells ability to sense and respond to environmental conditions such as nutrient availability. In order to coordinate cellular metabolism and strategize, the cell needs an exact perception of the dynamics of intra- and extra- cellular metabolites (Y. P. Wang & Lei, 2018). Simultaneously, nutrient-induced signaling plays a pivotal role in numerous human diseases like obesity, type 2 diabetes, cancer and ageing (Coughlan et al., 2014; Weidong Li et al., 2015; Salminen & Kaarniranta, 2012; Steinberg & Kemp, 2009). Therefore, unravelling the role of nutrients as signaling molecules and metabolites as well as their interconnectivity may provide a deeper understanding of how these conditions occur.

Yeast has long been used as a model organism for studying nutrient-induced signaling (Conrad et al., 2014a). Two major classes of nutrients include carbon and nitrogen. Carbon-induced signaling acts mainly through the PKA and SNF1 pathway while nitrogen-induced signaling acts through the mTOR pathway. The PKA pathway plays a major role in regulating growth by inducing ribosome biogenesis genes and inhibiting stress response genes(Broach, 2012). The SNF1 pathway is mainly active in low glucose conditions where it promotes respiratory metabolism, glycogen accumulation, gluconeogenesis and utilization of alternative carbon sources but it also controls cellular developmental processes such as meiosis and ageing (Ashrafi et al., 2000; Conrad et al., 2014a; Hedbacker & Carlson, 2008). The strongly conserved TORC1 pathway plays a crucial role in promoting anabolic processes and cell growth in response to nitrogen availability (Broach, 2012). Active TORC1 induces ribosomal protein and ribosome biogenesis gene expression (Lempiäinen et al., 2009; Marion et al., 2004) and represses transcription of genes containing STR and PDS elements in their promoter region (Lempiäinen et al., 2009). Despite the fact that Snf1, TORC1 and PKA pathways belong to the most well-studied pathways (Y. P. Wang & Lei, 2018), still, there is a lack of understanding both in the dynamics and the interactions leading to change in gene expression. It has been shown that glucose signaling is related to metabolism however the nature of this relationship remains unknown (Welkenhuysen et al., 2017). Numerous crosstalk mechanisms between these pathways have been described (Shashkova et al., 2015) and depending on their activity, they may influence the overall effect of the signaling process and thus the interaction with the

metabolism (Welkenhuysen et al., 2019). In order to better understand the impact of cell signaling on metabolism, a systems biology approach is often implemented (Nielsen, 2017).

Typically, Boolean models have been developed to study the crosstalk between the Snf1 pathway and the Snf3/Rgt2 pathway (Christensen et al., 2009) as well as the Snf1, cAMP-PKA, and Rgt2/Snf3 pathways (Welkenhuysen et al., 2019). In mammalian cells, Boolean models have been used to evaluate the conflicting hypothesis of the regulation of the mTOR pathway (Sulaimanov et al., 2017) and to study crosstalk between mTOR and MAPK signaling pathways (Siegle et al., 2018). Since, signaling systems are not always strictly Boolean in its nature, where location, combinations of post-translational modifications as well as other interaction plays a role, different Boolean frameworks for handling these complex interactions have been developed (Romers et al., 2020; Welkenhuysen et al., 2019). In contrast, metabolism, also in itself a complex process, is often studied using Flux Balance Analysis (FBA), that enables prediction of biochemical reaction fluxes, cellular growth on different environments and gene essentiality even for genome-scale metabolic models (GEMs) (Lu et al., 2019; Monk et al., 2017; Yilmaz & Walhout, 2017). A major limitation of the use of GEMs together with FBA is the high variability of flux distributions for a given cellular objective (Mahadevan & Schilling, 2003), as FBA solves largely underdetermined linear systems through optimization methods. To overcome this problem, experimentally measured exchange fluxes (uptake of nutrients and secretion of byproducts) are incorporated as numerical constraints, however, such measurements are not always available for a wide variety of organisms and growth conditions.

The concept of enzyme capacity constraints has been incorporated into FBA in order to reduce the phenotypic solution space (i.e. exclusion of flux distributions that are not biologically meaningful) and diminish its dependency on condition-dependent exchange fluxes datasets (Adadi et al., 2012; Beg et al., 2007; Bekiaris & Klamt, 2020; Massaiu et al., 2019; Nilsson & Nielsen, 2016; Sánchez et al., 2017).

Notably, a method to account for enzyme constraints, genome-scale models using kinetics and omics (GECKO) (Sánchez et al., 2017)has been developed. GECKO incorporates constraints on metabolic fluxes given by the maximum activity of enzymes, which are also constrained by a limited pool of protein in the cell. This method has refined predictions for growth on diverse environments, cellular response to genetic perturbations, and even predicted the Crabtree effect in *S. cerevisiae*'s metabolism, but also proven to be a helpful tool for probing protein allocation and enabled the integration of condition-dependent absolute proteomics data into metabolic networks (Massaiu et al., 2019; Sánchez et al., 2017).

Following the holistic view of systems biology, hybrid models allow us to take the next step and combine many different formalisms to study the interconnectivity and crosstalk spanning different scales and/or systems. For example, to quantify the contribution of the regulatory constraints of an *E.coli* genome-scale model, a steady-state regulatory flux balance analysis (SR-FBA) has been developed (Shlomi et al., 2007), further the diauxic shift in *S. cerevisiae* has been studied by CoRegFlux workflow integrating metabolic models and gene regulatory networks(Banos et al., 2017). To bypass the need for kinetic parameters, a FlexFlux tool has been developed where metabolic flux analyses using FBA have been constrained with steady-state values resulting from the regulatory network(Marmiesse et al., 2015). This strategy has also been used in a hybrid model of the *Mycobacterium tuberculosis* where the gene regulatory network was used to constrain the metabolic model to study the adaptation to the intra-host hypoxic environment(Bose et al., 2018). However, to further study the impact of signaling on the metabolism, the complexity of the signaling

systems itself and the crosstalk between interacting pathways need to be represented in a coherent manner.

To better understand the complex relationship between metabolism and signaling pathways, we created a hybrid model consisting of a Boolean module integrating the PKA, TORC1 and the Snf1 pathways as well as the known crosstalk between them and an enzyme-constrained module of *S. cerevisiae's* central carbon and energy metabolism (Figure 1). The backbone of the presented model is a framework for utilizing the complex Boolean representation of large-scale signaling systems to further constrain an enzyme-constrained model (ecModel), where the activity of the transcription factors resulting from the Boolean module was used to constrain an ecModel of the central carbon metabolism. The proposed hybrid model is capable of reproducing the regulatory effects that are associated with the Crabtree effect and glucose repression and have further showed a connection between glucose signaling and chronological lifespan by the regulation of NDE and NDI usage in respiring conditions. In addition, the model showed that during fermentation, enzyme utilization is the more important factor governing the protein allocation, while in low glucose conditions robustness and control is prioritized.

Figure 1. Schematic representation of the hybrid model. The hybrid model consists of a vector based Boolean module of nutrient signaling and a enzyme constrained module of the central carbon metabolism. The Boolean module is a dynamic module including Snf1, PKA and TORC1 pathway as well as crosstalk between them. The dynamic module reaches steady state and the activity of the transcription factors acts as input in a regulatory network constraining the enzyme constraint model of the central carbon metabolism. The solution is used to determine the activity of the Boolean input.

Results

Implemented Boolean signaling network is able to reproduce the general dynamics caused by glucose and nitrogen addition to starved cells

To verify the constructed Boolean model of nutrient-induced signaling pathways (Figure 2), cells were simulated from nitrogen and glucose starved conditions to nutrient rich conditions. The PKA pathway was activated upon glucose abundance via the small G proteins Ras and Gpa2. These proteins, in turn, activated the adenylate cyclase (AC) that induced processes leading to the activation of the catalytic subunit of PKA. Active PKA phosphorylated and therefore inactivated Rim15, thus the transcription factors Gis1, Msn2 and Msn4 became inactive.

The SNF1 pathway is active when glucose is limited, while the addition of glucose causes Snf1 inactivation resulting in the activation of the transcriptional repressor Mig1 and the deactivation of Adr1, Cat8 and Sip4. However, the inactivation of Adr1 happened prior to Snf1 inactivation. This is due to the implemented crosstalk with the PKA pathway, where activated PKA inhibits Adr1 activity (Cherry et al., 1989).

Nutrient availability activates the TOR complex 1 which in turn phosphorylates Sch9 and Sfp1 resulting in the repression of Rim15 phosphorylation and the expression of ribosomal genes respectively. No change was observed in the activity of PP2A-regulated transcription factors Rtg1, Rtg3, Gat2 and Gln2. However, during the 8^{th} iteration, PP2A was active. In addition, Sch9 was not the main regulator of Rim15 activity in our simulations since PKA was activated prior to Sch9 and acted independently to regulate Rim15, either due to a gap in the model or a lack of complexity in our understanding of the signalling system (Supplementary Information S1).

Figure 2. The Bolean module is a dynamic module including Snf1, PKA and TOR pathway as well as crosstalk between them. Crosstalk events between the pathways are depicted in grey. Unknown mechanisms are represented by dashed lines.

The Boolean model reveals interconnectivity and knowledge gaps in nutrient signaling pathways

To further investigate the impact of crosstalk in the Boolean model, knockouts of main components of each pathway (Snf1, Reg1, Tpk1-3 and Tor1,2) were simulated and compared to the wildtype in glc|nitr = 1|1 and glc|nitr = 0|0, see Figure S2. In nutrient-depleted conditions, only the Snf1 knockout had a significant impact. In the Snf1 pathway, Snf1 knockout affected all downstream targets leading to a transcription factor activity pattern that is usually observed in wildtype strains when glucose is available (Conrad et al., 2014b). It has been previously described that the phenotype of Snf1 mutants resembles the phenotype observed when the cAMP/PKA pathway is over-activated (Thompson-Jaeger et al., 1991). Although activation of the adenylate cyclase (AC) could be observed in the simulated knockout, PKA and the downstream targets were inactive due to the activity of the Krh proteins that inhibit PKA if no glucose is present in the Boolean model (T. Peeters et al., 2006). The Snf1 mutant showed defects in the TOR pathway upon glucose depletion leading to the activation of the PP2A phosphatase. The resulting activation of NCR and RTG genes and deactivation of ribosomal genes correspond to the phenotype one would expect if glucose but not nitrogen is available (Hughes Hallett et al., 2014) thus stressing the role of Snf1 in imparting the glucose state to the other nutrient-signaling pathways.

Under high nutrient availability, the Reg1 knockout showed almost the same effect on the SNF1 and TORC1 pathway as nutrient depletion. Only Adr1 activity was not affected which opposes the observations by Dombek and colleagues that described constitutive ADH2 expression in Reg1 mutant cells (Dombek et al., 1999).

An almost similar effect on the SNF1 and TORC1 pathways could be observed when Tpk1-3 knockout was simulated. This redundant effect was expected since impaired PKA activity was described to be associated with increased SNF1 activity(Barrett et al., 2012). Nevertheless, PKA knockout additionally induced Adr1 activation when SNF1-mediated activation could no longer be inhibited by PKA. The PKA knockout simulation showed strong effects on all three simulated pathways and may explain why strains lacking all three Tpk isoenzymes are inviable (Robertson & Fink, 1998).

The effects of Tor1 and 2 knockouts only affected the TORC1 signaling pathway. The simulated phenotype equalled the phenotype that is expected upon nitrogen depletion and glucose abundance and was therefore similar to the phenotype observed when simulating the Snf1 knockout in nutrient-starved cells. Besides, experimental observations revealed that impairing Tor1 and 2 function results in growth arrest in the early G1 phase of the cell cycle, as well as inhibition of translation initiation which are characteristics of nutrient, depleted cells entering stationary phase (Barbet et al., 1996). The fact that inactivation of TORC1 results in the inactivation of Sfp1 that regulates the expression of genes required for ribosomal biogenesis could be an indicator of this observation; however other TORC1-associated signaling mechanisms inducing translation initiation may likely be involved (Barbet et al., 1996).

The hybrid model improves predictions of individual proteins and reveals a connection between regulation and chronological ageing

To verify the ecModel performance, the predictions of exchange reaction fluxes at increasing dilution rates were compared against experimental data (Van Hoek et al., 1998) (Figure S3), predictions showed a median relative error of 9.82% in the whole range of dilution rates from 0 to 0.4 h^{-1}, spanning both respiratory and fermentative metabolic regimes. The hybrid model, including regulation, was further compared with the ecModel in their ability to predict protein abundances by comparing the predicted abundances to proteomics data from the literature in both respiratory and fermentative conditions (Doughty et al., 2020; Paulo et al., 2016). By adding the regulation layer, the prediction accuracy of individual protein abundances was drastically improved, reducing the mean absolute $\log_{10}$-transformed ratio between predicted and measured values (**r**) from 2.62 to 1.55 for respiration and from 3.56 to 2.32 for fermentation (Figure 3), which represents an average improvement in protein predictions by more than one order of magnitude for both conditions. Moreover, two sample Kolmogorov-Smirnov tests did not show significant statistical differences between model predictions and the available proteomics datasets. This large improvement is predominantly resulting from the utilization of more than one isoform for some reactions in the hybrid model in contrast to a pure ecModel, in which just the most efficient enzyme for a given reaction is used.

Pathway enrichment analysis of the proteins miss-predicted by more than one order of magnitude, by the hybrid model has been performed and showed that the superpathway of glucose fermentation was underpredicted for both respiration and fermentation (p-value of 1.398426e-7 and 7.002912e-5, respectively). Additionally, the superpathway of TCA cycle and glyoxylate cycle was underpredicted (p-value = 0.036267), whilst aerobic respiration and electron transport chain were significantly overpredicted (p-value = 2.857451e-23) in the fermentative state and the pentose phosphate pathway (p-value= 2.863892e-4) as well as glucose-6-phosphate biosynthesis (p-value= 0.019529) were underpredicted in respiration. A detailed comparison between the models as well as in-depth results from the protein predictions are available in Data file S1 and Supplementary Information S1.

To better understand which pathways and reactions are most affected by regulation, the metabolic flux distributions predicted by the hybrid model and the ecModel were compared. Larger flux differences arose for respiratory conditions, in which the average relative change in flux was 1.85 in contrast to 0.46 in fermentation (Data file S2), this result is heavily influenced by the amount of totally activated or deactivated fluxes by the hybrid model, 57 for respiration and 29 for fermentation (Figure 3, Data file S2). ecModels provide a network in which reversible metabolic reactions are split, creating separate reactions for the forward and backwards fluxes, thus distributions of net metabolic fluxes were also obtained and compared among models and conditions. As some enzymes are upregulated by the hybrid model even to levels that exceed the flux capacity of certain pathways (for a fixed growth rate), futile fluxes are expected to arise across the metabolic network.

Increased exchange fluxes for glucose, oxygen and acetate were observed in the respiration phase (Data file S2). Additionally, an increase in the overall flux through the pentose phosphate pathway as well as an induced use of NDE instead of only NDI, allowing for the utilization of cytosolic NADH to reduce oxygen demands in the oxidative phosphorylation pathway was detected and has previously been associated with chronological ageing (Wei Li et al., 2006). Increased flux on PCK, PDC, ALD2 and ACS, around the pyruvate branching point, led to an overall increased flux through the TCA cycle (Figure 3 and Data file S2). To balance the increased production of AMP by ACS the ADK reaction is also upregulated. Futile fluxes are induced by regulation in galactose metabolism (GAL7 and GAL10), lower glycolysis (TDH, PGK and ENO), TCA cycle (FUM and MDH), as well as

TKLa and PGM in the pentose phosphate pathway and ADH (Figure 3 and Data file S2) in respiration.

In the fermentation state, futile fluxes also occur in galactose metabolism (GAL7) as well as glycolysis (PGI, PGK, TPI and GPM), TAL1 in the pentose phosphate pathway and ACO in the TCA cycle (Figure S4 and Data file S2). Down-regulation of oxidative metabolism, increased uptake of glucose and increased flux through glycolysis were observed, which is consistent with the changes that have been attributed to glucose-induced repression during the long term Crabtree effect (de Alteriis et al., 2018) (Figure 3).

The control exerted by each enzyme on the global glucose uptake rate was investigated through the calculation of flux control coefficients (FCCs), allowing comparison of the distribution of metabolic control between the pure enzyme-constrained and hybrid model. In both conditions the FCCs obtained for hexokinases by the ecModel (HXK1 for respiration and HXK3 in fermentation) showed a value equal to 1, the highest value in their respective distributions, indicating that the overall glucose uptake rate is mostly governed by the activity of this enzymatic reaction step. In contrast, the constraints applied by the hybrid model distribute the control over the glucose uptake flux in a more even way across different enzymes and pathways, yielding FCCs of 0 for the different HXK isoforms in both metabolic regimes.

As a general trend, more FCCs with a high value (FCC>0.05) are obtained for fermentative conditions than for respiration, despite the use of the ecModel or hybrid model (Figure 3 and Data file S3). In the respiratory condition, the highest FCCs are concentrated in the oxidative phosphorylation pathway as well as around the branching point of pyruvate and PFK in glycolysis, whose activity is related to the connections between glycolysis and PP pathway. Moreover, the absence of glucose uptake control by lower glycolytic enzymes, and the prevalence of a non-zero FCC for PFK in both ecModel and hybrid model agrees with experimental evidence for mouse cell-lines in respiratory conditions (Tanner et al., 2018). For the fermentative condition the highest FCCs are concentrated in the TCA cycle. Similarly to the respiration case, non-zero FCCs are present in the reaction steps surrounding the connecting points of different pathways, such as PFK, FBA and TDH connecting glycolysis with the pentose phosphate pathway and reactions around pyruvate, which connect glycolysis with fermentation and the TCA cycle (Figure 3), this trend might indicate that in these branching points kinetic control is still a relevant mechanism governing fluxes.

Figure 3. (A) Absolute $\log_{10}$-transformed ratio between predicted and measured values in respiration and fermentation. The plot shows unregulated prediction from the ecModel that works on optimality principles and the regulation predictions from the hybrid model. (B) The regulated model forces the use of isoenzymes. Here we display the regulated (Hybrid model), the unregulated (ecModel) and the proteomics data for the isoenzymes catalysing the HXK reaction. In the lower panel the the core reactions in the metabolism under (C) respiration and (D) fermentation are shown. The fluxes are represented by the width of the connectors where dotted lines represent zero flux. The colour of the connectors represent the change in flux from the unregulated ecModel compared to the regulated hybrid model. The FCCs are represented in the figure where the unregulated case is depicted by circles and compared to the regulated case depicted in squares.

Deletion of the Snf1 in the hybrid model shows the importance of the Snf1 pathway in low glucose conditions and attributes the connection between regulation and chronological ageing to Snf1

To investigate how the individual signaling pathways contribute to changes in metabolic fluxes, the main component of each signaling pathway was deleted and flux changes were compared between the wild-type hybrid model and the knockout versions (Data file S4).

The Snf1 deletion was the only deletion showing any effect on the net fluxes in the respiratory condition (Figure S4) while the Reg1, PKA and TOR deletions showed effects in fermentation conditions, consistent with the deletion experiments done with the Boolean model. The different mutants in fermentation do not induce major changes in net fluxes, however, the enzyme usage profile differs across the different mutants. Notably, the largest changes in terms of futile fluxes were observed in the TPI reaction, repressed in respiration by the Snf1 pathway and activated in fermentative conditions by either the PKA or Reg1 pathways. In respiration, Snf1 is also responsible for the futile fluxes through GPM, PGI and reduces the futile fluxes trough FUM, MDH, PGM and GAL10. The model simulations show a less diverse use of isoenzymes in all knockouts, which is most likely due to the reduction in the complexity of the regulatory layer. Considering the inherent property of flux balance analysis, any reduction in the regulatory network will be closer to the optimal distribution in which just the most efficient isoforms are used.

The Snf1 deletion exhibits an overall decrease in the flux towards respiration and a large decrease in flux through PPP, showing also a relatively strong downregulation of enzymatic steps surrounding pyruvate. The most significant changes are observed in NDE and PCK that are turned off and ALD6 which is turned on, implying that the Snf1 pathway is responsible for changing the acetate production via ALD6 to acetate production via ALD2, resulting in increased production of cytosolic NADH to the expense of the NADPH, which is compensated by increasing the flux through the pentose phosphate pathway as well as the additional use of NDE.

Discussion

The effects of nutrient-induced signaling on metabolism play an important role in maintaining organismal homeostasis and consequently understanding human disease and ageing. To gain a better understanding of the interconnectivity between nutrient signaling and metabolism, we have developed a hybrid model by combining the Boolean and the enzyme constraint models using a regulatory network as a link. More specifically, we have implemented a Boolean signaling network that is responsive to glucose and nitrogen and an ecModel of yeast's central carbon metabolism. The proposed framework has been validated using available experimental data resulting in an increased predictive power on individual protein abundances in comparison to individual models alone. Further we were able to characterize the cells deviation from the optimal protein allocation and flux distribution profiles. The model is capable of reproducing the regulatory effects that are associated with the Crabtree effect and glucose repression. The model showed a connection between SNF1 signaling and chronological lifespan by the regulation of NDE and NDI usage in respiring conditions. In addition, the model showed that during fermentation, enzyme utilization is the more important factor governing the protein allocation, while in low glucose conditions robustness and control is prioritized.

The integration of regulation constraints is resulting in a highly constrained hybrid model. The downside of this approach is connected to the lack of information regarding the regulatory effects of transcription factor activation. In this work we assume a uniform proportional action for all gene targets, together with the other constraints of the model, resulting in a rather low effect on the regulatory action. Despite this, the hybrid model shows improved protein abundance predictive power and can qualitatively reproduce regulatory effects associated with glucose repression in

fermentation conditions, suggesting that with this framework we can gain novel insight into the interplay between signaling pathways and metabolism, however, any quantitively or definitive statements should be avoided. Another limitation is the inclusion of only the central carbon metabolism, a potential extension of this work would include the addition of pathways responsive to glucose signaling, like glycerol metabolism and fatty acid synthesis, enabling also the study of the regulatory effect on these pathways specifically with relatively few modifications in the hybrid model.

The hybrid model shows that under regulation the NADH to support the electron transport chain is partly coming from the cytosol with the help of the mitochondrial external NADH dehydrogenase, NDE2. Overexpression of NDI1, in contrast to NDE1, causes apoptosis-like cell death which can be repressed by growth on glucose-limited media (Wei Li et al., 2006). In our model regulation acts on both NDE and NDI which will lower the need for NDI1 expression and thus causing apoptosis-like cell death. The hybrid model gives the ability to determine that the Snf1 pathway alone is responsible for the shift to the additional use of NDE and NDI instead of only NDI. Snf1 is active in glucose-limited media and thus would help mitigate the phenotype of over expressed NDI1. With these result, we can connect Snf1 with the respiration-restricted apoptotic activity described by Wei Li et al and help explain how Snf1 is connected to chronological ageing (Wierman et al., 2017).

Futile fluxes in the cell have been examined previously within the constraints of osmotics, thermodynamics and enzyme utilization (Park et al., 2016b), where the osmotics are putting a ceiling on the allowed metabolite concentrations in the cell while thermodynamics govern the net fluxes through reactions. The induced futile fluxes can be explained by the fact that regulation included in the hybrid model will force the cell to use some enzymes even above its pathway flux requirements, adding robustness of metabolism to a constantly changing environment. The increase in flux in both forward and backward directions (i.e the increased futile flux through reactions) implies that these enzymes are working closer to their equilibrium and thus have a low flux control over the pathway flux, while enzymes with a strong forward flux have large flux control (Kacser et al., 1995). This feature is also displayed by our hybrid model, in which all enzymatic steps with induced futile fluxes exert null control over glucose uptake (FCCs = 0). More enzymes in a pathway working close to their equilibrium results in robustness against perturbations as well as allows the pathway to be controlled and regulated through a few enzymes, however, this happens at the expense of inefficient utilization of enzymes as the cell needs to spend more resources to sustain a pool of enzymes that are carrying both forward and backward fluxes (Noor et al., 2016; Park et al., 2016a). Our predictions of several glycolytic steps forced to operate closer to their equilibrium by regulation (high futile fluxes induced for TDH, PGK and ENO in respiration, and for TPI, PGK and GPM in fermentation) agree with experimental studies on *E. coli*, iBMK cells and *Clostridia cellulyticum*, which have suggested the utility of near-equilibrium glycolytic steps not just for providing robustness to environmental changes but also for enhancing metabolic energy yield (Park et al., 2019).

Computation of FCCs showed that in respiration the glucose flux is tightly dependent on the activity of the enzymatic steps in oxidative phosphorylation, a high-energy yield pathway. In contrast, in the fermentative condition flux control is split between PFK, PYK, PDC and several steps in the TCA cycle. Interestingly, the FCCs in TCA cycle are decreased by around the half after applying the regulatory constraints in the hybrid model, providing hints of the importance of enhancing robustness in this pathway at high growth rates due to increased demand of biomass precursors. The prevalence of the highest FCCs in fermentation for PFK, PYK and PDC (for both ecModel and hybrid model) indicate their important role as modulators of flux balance between glycolysis, PPP and fermentative

pathways at highly demanding conditions, suggesting that when entering fermentation, the cell sacrifices robustness to favor enzyme utilization.

Comparison of enzyme usage and flux distributions between models and across conditions reveals that the effects of regulation are generally stronger for the respiratory condition, causing the arisen of more and higher futile fluxes; turning on reaction steps that are not required by optimal metabolic allocation (purely ecModel); and inducing higher fold-changes into fluxes. These findings suggest that metabolic phenotypes are majorly shaped by regulatory constraints in low glucose conditions, whilst enzymatic constraints play a major role when glucose is not the limiting resource.

It was also found that the regulatory layer diminishes the strong flux control that hexokinase isoforms have over glucose consumption in both low and high glucose conditions to 0. The hexokinases in yeast, specially HXK2, have a central role in glucose signaling. It works both as an effector in the Snf1 pathway and also actively participates in the repression complex together with Mig1 in glucose repression during high glucose conditions (Vega et al., 2016). Intuitively, it would be practical if an enzyme having these central and diverse tasks in the cell would not have such a high FCC as can be seen with the ecModel. When small perturbations in enzyme activity or concentration have large effects on glucose consumptions, allocating this enzyme to other parts of the cell such as the nucleus while participating in the repression complex, would be energetically expensive. Given the central role of hexokinase in glucose signaling, this would be of interest for further investigation and future studies.

Overall, in this work, we have shown how the hybrid modeling framework integrating nutrient-sensing pathways and central carbon metabolism can not only improve individual model predictions but can also elucidate how single components in the dynamic signaling layer affect the steady-state metabolism. We tested our model against both respiring and fermenting conditions and could not only predict known phenomena but also find novel connections. This methodology can be used to connect both original and readily available models in yeast to look at the interactions between signaling and metabolism. This can be applied to genome-scale and on different subsystems of metabolism and for different signaling systems, for example, macronutrients or osmotic stress etc. The availability of genome-scale models of different organisms is constantly growing and with our increasing understanding of signaling systems and regulatory networks, the methodology developed in the course of this work can be adapted to many other organisms. Hybrid models, like the one proposed here, provides a framework for testing a different hypothesis, as we demonstrated by knocking out several components of the nutrient-induced signaling network. In summary, we developed a methodology to investigate intrinsically different systems, such as signaling and metabolism, in the same model gaining insight into how the interplay between them can have non-trivial effects.

Materials and methods

1.1 Boolean model of nutrient-induced signaling pathways

Based on an extensive literature review, a detailed topology of the nutrient-induced signaling pathways TORC1, SNF1 and PKA accounting also for their crosstalks was derived and formalized as a Boolean network model using a vector-based modelling approach (Welkenhuysen et al., 2019) **TORC1**: (Broach, 2012; Fernández-García et al., 2012; Hong et al., 2003; Kacherovsky et al., 2008; Leverentz & Reece, 2006; Ludin et al., 1998; MacPherson et al., 2006; Santangelo, 2006; Sanz et al., 2000; Schüller, 2003; Smith et al., 2011; Soontorngun et al., 2012; Sutherland et al., 2003; Turcotte et al., 2010; Westholm et al., 2008; Woods et al., 1994); **SNF1:** (Broek et al., 1987; Colombo et al.,

1998; Dihazi et al., 2003; Hu et al., 2010; Jones et al., 1991; Kataoka et al., 1985; Kraakman et al., 1999; Ma et al., 1999; Martínez-Pastor et al., 1996; Matsumoto et al., 1982; Nikawa et al., 1987; Pedruzzi et al., 2000; K. Peeters et al., 2017; T. Peeters et al., 2006; Portela et al., 2002; Rittenhouse et al., 1987; Robinson et al., 1987; Rolland et al., 2000; Sass et al., 1986; Schepers et al., 2012; Swinnen et al., 2006; K Tanaka et al., 1989, 1990; Kazuma Tanaka et al., 1990; T Toda et al., 1987; Takashi Toda et al., 1985, 1987); **PKA:** Bar-Peled et al., 2013; Beck & Hall, 1999; Binda et al., 2009; Bonfils et al., 2012; Broach, 2012; Conrad et al., 2014; Dilova, Aronova, Chen, & Powers, 2004; Dubouloz, Deloche, Wanke, Cameroni, & De Virgilio, 2005; Georis, Feller, Vierendeels, & Dubois, 2009; Hughes Hallett, Luo, & Capaldi, 2014; Kuruvilla, Shamji, & Schreiber, 2001; Lempiäinen et al., 2009; Liu & Butow, 1999; Marion et al., 2004; Reinke et al., 2004; Urban et al., 2007; Wanke et al., 2008; Yan, Shen, & Jiang, 2006; **crosstalks**: Barrett, Orlova, Maziarz, & Kuchin, 2012; Castermans et al., 2012; Cherry, Johnson, Dollard, Shuster, & Denis, 1989; Hughes Hallett et al., 2014; Nicastro et al., 2015; Wanke et al., 2008).

The model consists of four different components: metabolites, target genes, regulated enzymes and proteins. For the regulated enzymes, presence and phosphorylation state were considered whereas metabolites and target genes were only described by a single binary value indicating their presence and transcriptional state respectively. The state vectors were translated into a single binary value indicating the components' activity, allowing a better graphical depiction. In total, the model comprises 5 metabolites, 10 groups of target genes, 6 enzymes whose activity is altered upon nutrient signaling and 46 proteins belonging to PKA/cAMP, the SNF1 and the TORC1 pathway, for detailed description, see Supplementary Information S1 and Table S1-S6.

Availability of glucose and nitrogen was used as an input to the model and is implemented as one vector of binary values for each nutrient. This input enables to simulate the induction of signaling under different nutrient conditions, for instance the addition of glucose and nitrogen to starved cells is represented by the vector 0|1 for both nutrients respectively. Here, 0 represent the starved or low nutrient condition and 1 the nutrient-rich condition. Based on this input and the formulation of the Boolean rules, a cascade of state transitions is induced. The simulation was conducted using a synchronous updating scheme meaning that at each iteration, the state vectors are updated simultaneously. The algorithm stops if a Boolean steady state is reached at which no operation causes a change in the state vectors. This process is repeated for each pair of glucose and nitrogen availabilities whereby the reached steady state for each nutrient condition serves as an initial condition for the next nutrient condition.

Since for many of the included processes, no information on the mechanisms causing reversibility was available, especially a lack in the knowledge on phosphatases reverting phosphorylation was observed (Welkenhuysen *et al* 2019), gap-filling was conducted by including else-statements. This ensures that a component's state vector changes again e.g. if the conditions causing its phosphorylation are not fulfilled anymore. This gap-filling process guarantees the functionality of the Boolean model in both directions, meaning the simulation of state transitions occurring when nutrients (glucose and nitrogen) are added to nutrient-depleted cells as well as when cells are starved for the respective nutrients. Crosstalk mechanisms between the pathways were formulated as if-statements and can be switched off (0) or on (1). Furthermore, a simulation of knockouts of the pathways' components is possible by setting the value indicating their presence to 0.

Enzyme-constrained metabolic model

A reduced stoichiometric model of *Saccharomyces cerevisiae's* central carbon and energy metabolism, including metabolites, reactions, genes and their interactions accounting for glycolysis, TCA cycle, oxidative phosphorylation, pentose phosphate, Leloir and anaerobic excretion pathways, together with a representation of biomass formation, was taken as a network scaffold(Nilsson & Nielsen, 2016). The metabolic model was further enhanced with enzyme constraints using the GECKO toolbox v1.3.5 (Sánchez et al., 2017), which considers enzymes as part of metabolic reactions, as they are occupied by metabolites for a given amount of time that is inversely proportional to the enzyme's turnover number (k_{cat}). Therefore, enzymes are incorporated as new "pseudo metabolites" and usage pseudo reactions are also introduced in order to represent their connection to a limited pool of protein mass available for metabolic enzymes. Moreover, all reversible reactions are split into two reactions with opposite directionalities in the ecModel, in order to account for the enzyme demands of backwards fluxes. Several size metrics for the Boolean model, the metabolic network and its enzyme-constrained version (ecModel) are shown in Table 1.

As the obtained ecModel has the same structure as any metabolic stoichiometric model, in which metabolites and reactions are connected by a stoichiometric matrix, the technique of flux balance analysis (FBA) can be used for quantitative prediction of intracellular reaction fluxes (Orth et al., 2010). FBA assumes that the metabolic network operates on steady-state, i.e. no net accumulation of internal metabolites, due to the high turnover rate of metabolites when compared to cellular growth or environmental dynamics (Varma & Palsson, 1994), therefore, by setting mass balances around each intracellular metabolite a homogenous system of linear equations is obtained. The second major assumption of FBA is that metabolic phenotypes are defined by underlying organizational principles, therefore an objective function is set as a linear combination of reaction fluxes which allows to obtain a flux distribution by solving the following linear programming problem

$$\max: Z = C^T v$$

Subject to

$$S \cdot v = 0$$

$$lb \leq v \leq ub$$

Where C^T, is a transposed vector of integer coefficients for each flux in the objective function (Z); v, is the vector of reaction fluxes; S, is a stoichiometric matrix, representing metabolites as rows and reactions as columns; lb and ub are vectors of lower and upper bounds, respectively, for the reaction fluxes in the system. Additionally, the incorporation of enzyme constraints enables the connection between reaction fluxes and enzyme demands, which are constrained by the aforementioned pool of metabolic enzymes

$$v_i = \sum_j k_{cat_{ij}} \cdot e_j$$

$$\sum_j^p Mw_j \cdot e_j \leq f \cdot \sigma \cdot P_{tot}$$

Where $k_{cat_{ij}}$ is the turnover number of the enzyme j for the i-th reaction, as in some cases several enzymes can catalize the same reaction (isoenzymes); e_j, is the usage rate for the enzyme j in mmol/gDw h^{-1}; Mw_j, represents the molecular weight of the enzyme j, in mmol/g; P_{tot}, is the total

protein content in a yeast cell, corresponding to a value of 0.46 g_{prot}/gDw (Famili et al., 2003); f, is the fraction of the total cell proteome that is accounted for in our ecModel, 0.1732 when using the integrated dataset for *S. cerevisiae* in paxDB as a reference (M. Wang et al., 2015b); and σ being an average saturation factor for all enzymes in the model.

Table 1 Size metrics for the Boolean, original metabolic model and its enzyme-constrained version.

Boolean model	
Metabolites	5
Target gene groups	10
Enzyme PTMs	6
Proteins	46
Metabolic model	
Reactions	90
Metabolites	81
Genes	130
Cellular compartments	4
ecModel	
Reactions	324
Metabolites	111
Enzymes	127
Promiscuous enzymes	41
Reactions with isoenzymes	30
Enzyme complexes	11
Reactions w/Kcat	115

This simple modelling formalism enables the incorporation of complex enzyme-reaction relations into the ecModel due to its matrix formulation, such as isoenzymes, which are different enzymes able to catalyse the same reaction; promiscuous enzymes, enzymes that can catalyze more than one reaction; and enzyme complexes, several enzyme subunits all needed to catalyse a given reaction.

ecModel curation

As the ecModel was generated by the automated pipeline of the GECKO toolbox, several of its components were curated in order to achieve predictions that are in agreement with experimental data at different dilution rates. Data on exchange reaction fluxes at increasing dilution rates, spanning both respiration and fermentative metabolic regimes (Van Hoek et al., 1998) was used as a comparison

basis. Additionally, all unused genes in the original metabolic network were removed and gene rules for lactose and galactose metabolism were corrected according to manually curated entries for *S. cerevisiae* available at the Swiss-Prot database (Bateman, 2019). Gene rules and metabolites stoichiometries (P/O ratio) in the oxidative phosphorylation pathway were also corrected according to the consensus genome-scale network reconstruction, Yeast8 (Lu et al., 2019).

The average saturation factor for the enzymes in the model was fitted to a value of 0.48, which allows the prediction of the experimental critical dilution rate (i.e. the onset of fermentative metabolism) at 0.285 h^{-1}. ATP requirements for biomass production were fitted by minimization of the median relative error in the prediction of exchange fluxes for glucose, oxygen, CO_2 and ethanol across dilution rates (0 – 0.4 h^{-1}), resulting in a linear relation depending on biomass formation from 18 to 25 mmol per gDw for respiratory conditions and from 25 to 30 mmol per gDw for the fermentative regime.

Hybrid model

A hybrid model consists of the Boolean model connected with the ecModel trough a transcriptional layer that regulates its constraints on protein allocation (Figure 1). The active transcription factors act on the upper or lower bounds of the enzyme usage pseudo reaction depending on down- or up regulation, respectively. The magnitude of the induced perturbations is calculated according to previously calculated enzyme usage variability ranges, subject to a given growth rate and optimal glucose rate, expressed as

Upregulation:

$$lb_{e_i}^{reg} = e_i^{opt} + RF * \left(e_i^{max} - e_i^{min}\right)$$

Downregulation:

$$ub_{e_i}^{reg} = e_i^{opt} - RF * \left(e_i^{max} - e_i^{min}\right)$$

Where $lb_{e_i}^{reg}$ and $ub_{e_i}^{reg}$ represent the lower and upper bounds for the usage pseudoreaction of enzyme *i* in the regulated model; e_i^{opt}, is a parsimonious usage for enzyme *i* for a given growth and glucose uptake rates; RF, corresponds to a regulation factor between 0 and 1; e_i^{max} and e_i^{min} are the maximum and minimum allowable usages for enzyme *i* under the specified conditions.

A distribution of parsimonious enzyme usages is obtained by applying the rationale of the parsimonious FBA technique (Lewis et al., 2010), which explicitly minimizes the total protein burden that sustains a given metabolic state (i.e. fixed growth and nutrient uptake rates).

To connect the transcription factor activity with gene regulation we extracted regulation information from YEASTRACT and set a regulation level of 5% of the enzyme usage variability range for the simulations. When several transcription factors affect the same gene, the effects are summed up and the resulting sum is used as a basis for constraint. For example, if a gene is downregulated by two transcription factors (-2) and upregulated by one transcription factor (+1), the net sum would be (-1), thus the gene will be downregulated. In our model, an absolute sum higher than 1 will not cause a stronger regulation, as this additive process is just implemented to define the directionality of a regulatory effect.

2.5 Enzyme usage variability analysis

As metabolic networks are highly redundant and interconnected, the use of purely stoichiometric constraints usually leads to an underdetermined system with infinite solutions (Kauffman et al., 2003), in a typical FBA problem it is common that even for an optimal value of the objective function, several reactions in the network can take any value within a "feasible" range, such ranges can be explored by flux variability analysis (Mahadevan & Schilling, 2003).

In this study, enzyme usage variability ranges for all of the individual enzymes are calculated by fixing a minimal glucose uptake flux, for a given fixed dilution rate, and then running sequential maximization and minimization for each enzyme usage pseudo reaction.

$$enzyme\ usage\ variability\ range = e_i^{max} - e_i^{min}$$

Subject to:

$$v_{Glc_{IN}} = lb_{Glc_{IN}} = ub_{Glc_{IN}} = v_{Glc_{IN}}$$

$$v_{bio} = lb_{bio} = ub_{bio} = D_{rate}$$

This approach allows the identification of enzymes that are either tightly constrained, highly variable or even not usable at optimal levels of biomass yield.

Simulations

Cellular growth on chemostat conditions, at varying dilution rates from 0 to 0.4 h^{-1}, was simulated with the multiscale model by the following sequence of steps:

1. Initially, the desired dilution rate is set as both lower and upper bounds for the growth pseudo reaction and the glucose uptake rate is minimized, assuming that cells maximize biomass production yield when glucose is limited (Oliveira et al., 2005; Schuetz et al., 2007)

$$\min: \quad v_{Glc_{IN}}$$

Subject to

$$D_{rate} \leq v_{bio} \leq D_{rate}$$

2. The obtained optimal uptake rate ($v_{Glc_{IN}}^{min}$) is then used as a basis to estimate a range of uptake flux to further constrain the ecModel.

$$v_{Glc_{IN}}^{min} \leq v_{Glc_{IN}} \leq (1 + SF) * v_{Glc_{IN}}^{min}$$

As $v_{Glc_{IN}}^{min}$ represents the minimum uptake rate allowed by the stoichiometric and enzymatic constraints of the metabolic network, possible deviations from optimal behaviour may be induced by regulatory circuits. In order to allow the Boolean model to reallocate enzyme levels a suboptimality factor (SF) of 15% was used to set an upper bound for $v_{Glc_{IN}}$.

3. The ecModel is connected to the glucose-sensing Boolean model through the glucose uptake rate. At the critical dilution rate, the glucose uptake rate obtained by the ecModel is 3.2914 mmol/gDw h, this value is used as a threshold to define a "low" or "high" glucose level input in the Boolean model,

represented as 0 and 1, respectively. For each dilution rate, the initial value of $v_{Glc_{IN}}^{min}$ is calculated and fed to the regulatory network, which runs a series of synchronous update steps until a steady-state is reached.

4. At steady state, the regulatory network indicates the enzyme usages that should be up and downregulated, for which new usage bounds are set as described above.

5. A final FBA simulation is run by minimizing the glucose uptake rate, subject to a fixed dilution rate and the newly regulated enzyme usage bounds.

Gene deletions can also be set in the Boolean module and will result in activation or inactivation of transcription factors which then affect the constraints on the FBA model. We ran four simulations of deletion strains as follows: TOR1 and TOR2 (TOR deletion), Snf1 (SNF1 deletion), Tpk1, Tpk2 and Tpk3 (PKA deletion) and Reg1(Reg1 deletion).

Proteomics analysis

Protein abundance data on respiratory and fermentative conditions were compared to protein usage predictions by the hybrid model in order to assess its performance. For the respiration phase, absolute protein abundances were taken from a study of yeast growing under glucose-limited chemostat conditions at 30°C on minimal mineral medium with a dilution rate of 0.1 h^{-1} (Doughty et al., 2020).

For the fermentation phase, a proteomics dataset was taken from a batch culture using minimal media with 2% glucose and harvested at an optical density (OD) of 0.6 (Paulo et al., 2016). The dataset given as relative abundances was then rescaled to relative protein abundances in the whole-cell according to integrated data available for *S. cerevisiae* in PaxDB (M. Wang, Herrmann, Simonovic, Szklarczyk, & von Mering, 2015), and finally converted to absolute units of mmol/gDw using the "total protein approach" (Wiśniewski & Rakus, 2014).

We used three metrics for comparing the simulations with the proteomics data, the Pearson correlation coefficient (PCC), two-sample Kolmogorov-Smirnov (KS) test and the mean of the absolute $\log_{10}$-transformed ratios between predicted and measured values (r). The PCC and the significance of the PCC were determined by a permutation test of n=2000. Pathway enrichments were done using YeastMine (Balakrishnan et al., 2012) with the Holm-Bonferroni test correction and a max p-value of 0.05.

Flux control coefficients

In order to investigate the relationship between enzyme activities and a given metabolic flux, control coefficients can be calculated for each enzyme in the model according to the definition given by metabolic control analysis (MCA) (Kacser et al., 1995):

$$FCC_{ij} = \frac{a_i}{v_j}\frac{\partial v_j}{\partial a_i}$$

In which $a_i = k_{cat_{ij}} e_i$ represents the activity of the *i-th* enzyme and v_j is the flux carried by the *j-th* reaction. These coefficients represent the sensitivity of a given metabolic flux to perturbations on enzyme activities, providing a quantitative measure on the control that each enzyme exerts on specific fluxes.

As ecModels include enzyme activities explicitly in their structure, flux control coefficients can be approximated by inducing small perturbations on individual enzyme usages:

$$FCC_{ij} \approx \frac{k_{cat_{ij}} e_i}{v_j} \frac{\Delta v_j}{\Delta \left(k_{cat_{ij}} e_i \right)}$$

In our hybrid model, perturbations on individual enzyme usages (e_i) are induced in relation to a parsimonious usage (e_i^*) which is compatible with a given set of constraints

$$FCC_{ij} = \frac{e_i^*}{v_j^*} \frac{\Delta v_j}{\Delta (e_i - e_i^*)}$$

Perturbations equivalent to 0.1% of the parsimonious usage are used for each enzyme. For those cases in which the previously applied constraints do not allow such modification in a given enzyme usage, their activity is then perturbed by operating on the corresponding turnover number for the enzyme-reaction pair ($k^*_{cat_{ij}} = 0.001 * k_{cat_{ij}}$) in order to simulate a perturbation in their overall activity.

The model, code and datasets used for this study can be found in the GitHub repository YeastHybridModelingFramework https://github.com/cvijoviclab/YeastHybridModelingFramework.

Acknowledgments

We would like to thank members of the Hohmann, Nielsen and Cvijovic labs for valuable input. Special thanks to Avlant Nilsson for his contributions to the curation of the original metabolic network used in this study and valuable discussions on the role of enzyme constraints.

Funding

This work was supported by the Swedish Research Council (VR2016-03744) to SH, the Swedish Agency for Strategic Research (Grant Nr. FFL15-0238) to MC and European Union's Horizon 2020 research and innovation program, project CHASSY (grant agreement 720824) to ID. Part of this work was funded by the Novo Nordisk Foundation (grant no. NNF10CC1016517) and the Knut and Alice Wallenberg Foundation.

Supplorting Information

SI. Supporting information. Includes detailed description of mechanisms reflected in the Boolean model of nutrient signalling.

References

Adadi, R., Volkmer, B., Milo, R., Heinemann, M., & Shlomi, T. (2012). Prediction of microbial growth rate versus biomass yield by a metabolic network with kinetic parameters. *PLoS Computational Biology*, *8*(7). https://doi.org/10.1371/journal.pcbi.1002575

Ashrafi, K., Lin, S. S., Manchester, J. K., & Gordon, J. I. (2000). Sip2p and its partner Snf1p kinase affect aging in S. cerevisiae. *Genes and Development*, *14*(15), 1872–1885.

https://doi.org/10.1101/gad.14.15.1872

Balakrishnan, R., Park, J., Karra, K., Hitz, B. C., Binkley, G., Hong, E. L., Sullivan, J., Micklem, G., & Cherry, J. M. (2012). YeastMine--an integrated data warehouse for Saccharomyces cerevisiae data as a multipurpose tool-kit. *Database : The Journal of Biological Databases and Curation*, *2012*, bar062. https://doi.org/10.1093/database/bar062

Banos, D. T., Trébulle, P., & Elati, M. (2017). Integrating transcriptional activity in genome-scale models of metabolism. *BMC Systems Biology*, *11*(Suppl 7). https://doi.org/10.1186/s12918-017-0507-0

Bar-Peled, L., Chantranupong, L., Cherniack, A. D., Chen, W. W., Ottina, K. A., Grabiner, B. C., Spear, E. D., Carter, S. L., Meyerson, M., & Sabatini, D. M. (2013). A tumor suppressor complex with GAP activity for the Rag GTPases that signal amino acid sufficiency to mTORC1. *Science*, *340*(6136), 1100–1106. https://doi.org/10.1126/science.1232044

Barbet, N. C., Schneider, U., Helliwell, S. B., Stansfield, I., Tuite, M. F., & Hall, M. N. (1996). TOR controls translation initiation and early G1 progression in yeast. *Molecular Biology of the Cell*, *7*(1), 25–42. https://doi.org/10.1091/mbc.7.1.25

Barrett, L., Orlova, M., Maziarz, M., & Kuchin, S. (2012). Protein kinase a contributes to the negative control of SNF1 protein kinase in saccharomyces cerevisiae. *Eukaryotic Cell*, *11*(2), 119–128. https://doi.org/10.1128/EC.05061-11

Bateman, A. (2019). UniProt: A worldwide hub of protein knowledge. *Nucleic Acids Research*. https://doi.org/10.1093/nar/gky1049

Beck, T., & Hall, M. N. (1999). The TOR signalling pathway controls nuclear localization of nutrient- regulated transcription factors. *Nature*, *402*(6762), 689–692. https://doi.org/10.1038/45287

Beg, Q. K., Vazquez, A., Ernst, J., de Menezes, M. A., Bar-Joseph, Z., Barabási, A. L., & Oltvai, Z. N. (2007). Intracellular crowding defines the mode and sequence of substrate uptake by Escherichia coli and constrains its metabolic activity. *Proceedings of the National Academy of Sciences of the United States of America*, *104*(31), 12663–12668. https://doi.org/10.1073/pnas.0609845104

Bekiaris, P. S., & Klamt, S. (2020). Automatic construction of metabolic models with enzyme constraints. *BMC Bioinformatics*. https://doi.org/10.1186/s12859-019-3329-9

Binda, M., Péli-Gulli, M. P., Bonfils, G., Panchaud, N., Urban, J., Sturgill, T. W., Loewith, R., & De Virgilio, C. (2009). The Vam6 GEF Controls TORC1 by Activating the EGO Complex. *Molecular Cell*, *35*(5), 563–573. https://doi.org/10.1016/j.molcel.2009.06.033

Bonfils, G., Jaquenoud, M., Bontron, S., Ostrowicz, C., Ungermann, C., & De Virgilio, C. (2012). Leucyl-tRNA Synthetase Controls TORC1 via the EGO Complex. *Molecular Cell*, *46*(1), 105–110. https://doi.org/10.1016/j.molcel.2012.02.009

Bose, T., Das, C., Dutta, A., Mahamkali, V., Sadhu, S., & Mande, S. S. (2018). Understanding the role of interactions between host and Mycobacterium tuberculosis under hypoxic condition: an

in silico approach. *BMC Genomics*, *19*(1), 555. https://doi.org/10.1186/s12864-018-4947-8

Broach, J. R. (2012). Nutritional control of growth and development in yeast. In *Genetics* (Vol. 192, Issue 1, pp. 73–105). Genetics Society of America. https://doi.org/10.1534/genetics.111.135731

Broek, D., Toda, T., Michaeli, T., Levin, L., Birchmeier, C., Zoller, M., Powers, S., & Wigler, M. (1987). The S. cerevisiae CDC25 gene product regulates the RAS/adenylate cyclase pathway. *Cell*, *48*(5), 789–799. https://doi.org/10.1016/0092-8674(87)90076-6

Castermans, D., Somers, I., Kriel, J., Louwet, W., Wera, S., Versele, M., Janssens, V., & Thevelein, J. M. (2012). Glucose-induced posttranslational activation of protein phosphatases PP2A and PP1 in yeast. *Cell Research*, *22*(6), 1058–1077. https://doi.org/10.1038/cr.2012.20

Cherry, J. R., Johnson, T. R., Dollard, C., Shuster, J. R., & Denis, C. L. (1989). Cyclic AMP-dependent protein kinase phosphorylates and inactivates the yeast transcriptional activator ADR1. *Cell*, *56*(3), 409–419. https://doi.org/10.1016/0092-8674(89)90244-4

Christensen, T. S., Oliveira, A. P., & Nielsen, J. (2009). Reconstruction and logical modeling of glucose repression signaling pathways in Saccharomyces cerevisiae. *BMC Systems Biology*, *3*, 7. https://doi.org/10.1186/1752-0509-3-7

Colombo, S., Ma, P., Cauwenberg, L., Winderickx, J., Crauwels, M., Teunissen, A., Nauwelaers, D., de Winde, J. H., Gorwa, M. F., Colavizza, D., & Thevelein, J. M. (1998). Involvement of distinct G-proteins, Gpa2 and Ras, in glucose- and intracellular acidification-induced cAMP signalling in the yeast Saccharomyces cerevisiae. *The EMBO Journal*, *17*(12), 3326–3341. https://doi.org/10.1093/emboj/17.12.3326

Conrad, M., Schothorst, J., Kankipati, H. N., Van Zeebroeck, G., Rubio-Texeira, M., & Thevelein, J. M. (2014a). Nutrient sensing and signaling in the yeast Saccharomyces cerevisiae. *FEMS Microbiology Reviews*, *38*(2), 254–299. https://doi.org/10.1111/1574-6976.12065

Conrad, M., Schothorst, J., Kankipati, H. N., Van Zeebroeck, G., Rubio-Texeira, M., & Thevelein, J. M. (2014b). Nutrient sensing and signaling in the yeast Saccharomyces cerevisiae. In *FEMS Microbiology Reviews* (Vol. 38, Issue 2, pp. 254–299). Wiley-Blackwell. https://doi.org/10.1111/1574-6976.12065

Coughlan, K. A., Valentine, R. J., Ruderman, N. B., & Saha, A. K. (2014). AMPK activation: A therapeutic target for type 2 diabetes? In *Diabetes, Metabolic Syndrome and Obesity: Targets and Therapy* (Vol. 7, pp. 241–253). Dove Press. https://doi.org/10.2147/DMSO.S43731

de Alteriis, E., Cartenì, F., Parascandola, P., Serpa, J., & Mazzoleni, S. (2018). Revisiting the Crabtree/Warburg effect in a dynamic perspective: a fitness advantage against sugar-induced cell death. In *Cell Cycle* (Vol. 17, Issue 6, pp. 688–701). https://doi.org/10.1080/15384101.2018.1442622

Dihazi, H., Kessler, R., & Eschrich, K. (2003). Glucose-induced stimulation of the Ras-cAMP pathway in yeast leads to multiple phosphorylations and activation of 6-phosphofructo-2-kinase. *Biochemistry*, *42*(20), 6275–6282. https://doi.org/10.1021/bi034167r

Dilova, I., Aronova, S., Chen, J. C. Y., & Powers, T. (2004). Tor signaling and nutrient-based signals

converge on Mks1p phosphorylation to regulate expression of Rtg1p·Rtg3p-dependent target genes. *Journal of Biological Chemistry*, *279*(45), 46527–46535. https://doi.org/10.1074/jbc.M409012200

Dombek, K. M., Voronkova, V., Raney, A., & Young, E. T. (1999). Functional analysis of the yeast Glc7-binding protein Reg1 identifies a protein phosphatase type 1-binding motif as essential for repression of ADH2 expression. *Molecular and Cellular Biology*, *19*(9), 6029–6040. https://doi.org/10.1128/mcb.19.9.6029

Doughty, T. W., Domenzain, I., Millan-Oropeza, A., Montini, N., de Groot, P. A., Pereira, R., Nielsen, J., Henry, C., Daran, J. M. G., Siewers, V., & Morrissey, J. P. (2020). Stress-induced expression is enriched for evolutionarily young genes in diverse budding yeasts. *Nature Communications*. https://doi.org/10.1038/s41467-020-16073-3

Dubouloz, F., Deloche, O., Wanke, V., Cameroni, E., & De Virgilio, C. (2005). The TOR and EGO protein complexes orchestrate microautophagy in yeast. *Molecular Cell*, *19*(1), 15–26. https://doi.org/10.1016/j.molcel.2005.05.020

Famili, I., Forster, J., Nielsen, J., & Palsson, B. Ø. (2003). Saccharomyces cerevisiae phenotypes can be predicted by using constraint-based analysis of a genome-scale reconstructed metabolic network. *Proceedings of the National Academy of Sciences of the United States of America*, *100*(23), 13134–13139. https://doi.org/10.1073/pnas.2235812100

Fernández-García, P., Peláez, R., Herrero, P., & Moreno, F. (2012). Phosphorylation of Yeast Hexokinase 2 Regulates Its Nucleocytoplasmic Shuttling *. *The Journal of Biological Chemistry*. https://doi.org/10.1074/jbc.M112.401679

Georis, I., Feller, A., Vierendeels, F., & Dubois, E. (2009). The Yeast GATA Factor Gat1 Occupies a Central Position in Nitrogen Catabolite Repression-Sensitive Gene Activation. *Molecular and Cellular Biology*, *29*(13), 3803–3815. https://doi.org/10.1128/mcb.00399-09

Hedbacker, K., & Carlson, M. (2008). SNF1/AMPK pathways in yeast. In *Frontiers in Bioscience* (Vol. 13, Issue 7, pp. 2408–2420). NIH Public Access. https://doi.org/10.2741/2854

Hong, S. P., Leiper, F. C., Woods, A., Carling, D., & Carlson, M. (2003). Activation of yeast Snf1 and mammalian AMP-activated protein kinase by upstream kinases. *Proceedings of the National Academy of Sciences of the United States of America*, *100*(15), 8839–8843. https://doi.org/10.1073/pnas.1533136100

Hu, Y., Liu, E., Bai, X., & Zhang, A. (2010). The localization and concentration of the PDE2-encoded high-affinity cAMP phosphodiesterase is regulated by cAMP-dependent protein kinase A in the yeast Saccharomyces cerevisiae. *FEMS Yeast Research*, *10*(2), 177–187. https://doi.org/10.1111/j.1567-1364.2009.00598.x

Hughes Hallett, J. E., Luo, X., & Capaldi, A. P. (2014). State transitions in the TORC1 signaling pathway and information processing in Saccharomyces cerevisiae. *Genetics*, *198*(2), 773–786. https://doi.org/10.1534/genetics.114.168369

Jones, S., Vignais, M. L., & Broach, J. R. (1991). The CDC25 protein of Saccharomyces cerevisiae promotes exchange of guanine nucleotides bound to ras. *Molecular and Cellular Biology*, *11*(5),

2641–2646. https://doi.org/10.1128/mcb.11.5.2641

Kacherovsky, N., Tachibana, C., Amos, E., Fox, D., & Young, E. T. (2008). Promoter binding by the Adr1 transcriptional activator may be regulated by phosphorylation in the DNA-binding region. *PLoS ONE*, *3*(9). https://doi.org/10.1371/journal.pone.0003213

Kacser, H., Burns, J. A., & Fell, D. A. (1995). The control of flux. *Biochemical Society Transactions*. https://doi.org/10.1042/bst0230341

Kataoka, T., Broek, D., & Wigler, M. (1985). DNA sequence and characterization of the S. cerevisiae gene encoding adenylate cyclase. *Cell*, *43*(2 PART 1), 493–505. https://doi.org/10.1016/0092-8674(85)90179-5

Kauffman, K. J., Prakash, P., & Edwards, J. S. (2003). Advances in flux balance analysis. In *Current Opinion in Biotechnology*. https://doi.org/10.1016/j.copbio.2003.08.001

Kraakman, L., Lemaire, K., Ma, P., Teunlssen, A. W. R. H., Donaton, M. C. V., Van Dijck, P., Winderickx, J., De Winde, J. H., & Thevelein, J. M. (1999). A Saccharomyces cerevisiae G-protein coupled receptor, Gpr1, is specifically required for glucose activation of the cAMP pathway during the transition to growth on glucose. *Molecular Microbiology*, *32*(5), 1002–1012. https://doi.org/10.1046/j.1365-2958.1999.01413.x

Kuruvilla, F. G., Shamji, A. F., & Schreiber, S. L. (2001). Carbon- and nitrogen-quality signaling to translation are mediated by distinct GATA-type transcription factors. *Proceedings of the National Academy of Sciences of the United States of America*, *98*(13), 7283–7288. https://doi.org/10.1073/pnas.121186898

Lempiäinen, H., Uotila, A., Urban, J., Dohnal, I., Ammerer, G., Loewith, R., & Shore, D. (2009). Sfp1 Interaction with TORC1 and Mrs6 Reveals Feedback Regulation on TOR Signaling. *Molecular Cell*, *33*(6), 704–716. https://doi.org/10.1016/j.molcel.2009.01.034

Leverentz, M. K., & Reece, R. J. (2006). Phosphorylation of Zn(II)2Cys6 proteins: A cause or effect of transcriptional activation? *Biochemical Society Transactions*, *34*(5), 794–797. https://doi.org/10.1042/BST0340794

Lewis, N. E., Hixson, K. K., Conrad, T. M., Lerman, J. A., Charusanti, P., Polpitiya, A. D., Adkins, J. N., Schramm, G., Purvine, S. O., Lopez-Ferrer, D., Weitz, K. K., Eils, R., König, R., Smith, R. D., & Palsson, B. (2010). Omic data from evolved E. coli are consistent with computed optimal growth from genome-scale models. *Molecular Systems Biology*, *6*. https://doi.org/10.1038/msb.2010.47

Li, Wei, Sun, L., Liang, Q., Wang, J., Mo, W., & Zhou, B. (2006). Yeast AMID homologue Ndi1p displays respiration-restricted apoptotic activity and is involved in chronological aging. *Molecular Biology of the Cell*, *17*(4), 1802–1811. https://doi.org/10.1091/mbc.E05-04-0333

Li, Weidong, Saud, S. M., Young, M. R., Chen, G., & Hua, B. (2015). Targeting AMPK for cancer prevention and treatment. *Oncotarget*, *6*(10), 7365–7378. https://doi.org/10.18632/oncotarget.3629

Liu, Z., & Butow, R. A. (1999). A Transcriptional Switch in the Expression of Yeast Tricarboxylic

Acid Cycle Genes in Response to a Reduction or Loss of Respiratory Function. *Molecular and Cellular Biology*, *19*(10), 6720–6728. https://doi.org/10.1128/mcb.19.10.6720

Lu, H., Li, F., Sánchez, B. J., Zhu, Z., Li, G., Domenzain, I., Marcišauskas, S., Anton, P. M., Lappa, D., Lieven, C., Beber, M. E., Sonnenschein, N., Kerkhoven, E. J., & Nielsen, J. (2019). A consensus S. cerevisiae metabolic model Yeast8 and its ecosystem for comprehensively probing cellular metabolism. *Nature Communications*, *10*(1), 1–13. https://doi.org/10.1038/s41467-019-11581-3

Ludin, K., Jiang, R., & Carlson, M. (1998). Glucose-regulated interaction of a regulatory subunit of protein phosphatase 1 with the Snf1 protein kinase in Saccharomyces cerevisiae. *Proceedings of the National Academy of Sciences of the United States of America*, *95*(11), 6245–6250. https://doi.org/10.1073/pnas.95.11.6245

Ma, P., Wera, S., Van Dijck, P., & Thevelein, J. M. (1999). The PDE1-encoded low-affinity phosphodiesterase in the yeast Saccharomyces cerevisiae has a specific function in controlling agonist- induced cAMP signaling. *Molecular Biology of the Cell*, *10*(1), 91–104. https://doi.org/10.1091/mbc.10.1.91

MacPherson, S., Larochelle, M., & Turcotte, B. (2006). A Fungal Family of Transcriptional Regulators: the Zinc Cluster Proteins. *Microbiology and Molecular Biology Reviews*, *70*(3), 583–604. https://doi.org/10.1128/mmbr.00015-06

Mahadevan, R., & Schilling, C. H. (2003). The effects of alternate optimal solutions in constraint-based genome-scale metabolic models. *Metabolic Engineering*, *5*(4), 264–276. https://doi.org/10.1016/j.ymben.2003.09.002

Marion, R. M., Regev, A., Segal, E., Barash, Y., Koller, D., Friedman, N., & O'Shea, E. K. (2004). Sfp1 is a stress- and nutrient-sensitive regulator of ribosomal protein gene expression. *Proceedings of the National Academy of Sciences of the United States of America*, *101*(40), 14315–14322. https://doi.org/10.1073/pnas.0405353101

Marmiesse, L., Peyraud, R., & Cottret, L. (2015). FlexFlux: combining metabolic flux and regulatory network analyses. *BMC Systems Biology*, *9*(1), 93. https://doi.org/10.1186/s12918-015-0238-z

Martínez-Pastor, M. T., Marchler, G., Schüller, C., Marchler-Bauer, A., Ruis, H., & Estruch, F. (1996). The Saccharomyces cerevisiae zinc finger proteins Msn2p and Msn4p are required for transcriptional induction through the stress response element (STRE). *The EMBO Journal*, *15*(9), 2227–2235. https://doi.org/10.1002/j.1460-2075.1996.tb00576.x

Massaiu, I., Pasotti, L., Sonnenschein, N., Rama, E., Cavaletti, M., Magni, P., Calvio, C., & Herrgård, M. J. (2019). Integration of enzymatic data in Bacillus subtilis genome-scale metabolic model improves phenotype predictions and enables in silico design of poly-γ-glutamic acid production strains. *Microbial Cell Factories*. https://doi.org/10.1186/s12934-018-1052-2

Matsumoto, K., Uno, I., Toh-E, A., Ishikawa, T., & Oshima, Y. (1982). Cyclic AMP may not be involved in catabolite repression in Saccharomyes cerevisiae: evidence from mutants capable of utilizing it as an adenine source. *Journal of Bacteriology*, *150*(1), 277–285. http://www.ncbi.nlm.nih.gov/pubmed/6277865

Monk, J. M., Lloyd, C. J., Brunk, E., Mih, N., Sastry, A., King, Z., Takeuchi, R., Nomura, W., Zhang, Z., Mori, H., Feist, A. M., & Palsson, B. O. (2017). iML1515, a knowledgebase that computes Escherichia coli traits. In *Nature Biotechnology* (Vol. 35, Issue 10, pp. 904–908). https://doi.org/10.1038/nbt.3956

Nicastro, R., Tripodi, F., Gaggini, M., Castoldi, A., Reghellin, V., Nonnis, S., Tedeschi, G., & Coccetti, P. (2015). Snf1 phosphorylates adenylate cyclase and negatively regulates protein kinase A-dependent transcription in Saccharomyces cerevisiae. *Journal of Biological Chemistry*, *290*(41), 24715–24726. https://doi.org/10.1074/jbc.M115.658005

Nielsen, J. (2017). Systems Biology of Metabolism. *Annual Review of Biochemistry*. https://doi.org/10.1146/annurev-biochem-061516-044757

Nikawa, J., Sass, P., & Wigler, M. (1987). Cloning and characterization of the low-affinity cyclic AMP phosphodiesterase gene of Saccharomyces cerevisiae. *Molecular and Cellular Biology*, *7*(10), 3629–3636. https://doi.org/10.1128/mcb.7.10.3629

Nilsson, A., & Nielsen, J. (2016). Metabolic Trade-offs in Yeast are Caused by F1F0-ATP synthase. *Scientific Reports*, *6*, 1–11. https://doi.org/10.1038/srep22264

Noor, E., Flamholz, A., Bar-Even, A., Davidi, D., Milo, R., & Liebermeister, W. (2016). The Protein Cost of Metabolic Fluxes: Prediction from Enzymatic Rate Laws and Cost Minimization. *PLoS Computational Biology*. https://doi.org/10.1371/journal.pcbi.1005167

Oliveira, A. P., Nielsen, J., & Förster, J. (2005). Modeling Lactococcus lactis using a genome-scale flux model. *BMC Microbiology*. https://doi.org/10.1186/1471-2180-5-39

Orth, J. D., Thiele, I., & Palsson, B. Ø. (2010). What is flux balance analysis? *Nature Biotechnology*, *28*(3), 245–248. https://doi.org/10.1038/nbt.1614

Park, J. O., Rubin, S. A., Xu, Y. F., Amador-Noguez, D., Fan, J., Shlomi, T., & Rabinowitz, J. D. (2016a). Metabolite concentrations, fluxes and free energies imply efficient enzyme usage. *Nature Chemical Biology*, *12*(7), 482–489. https://doi.org/10.1038/nchembio.2077

Park, J. O., Rubin, S. A., Xu, Y. F., Amador-Noguez, D., Fan, J., Shlomi, T., & Rabinowitz, J. D. (2016b). Metabolite concentrations, fluxes and free energies imply efficient enzyme usage. *Nature Chemical Biology*, *12*(7), 482–489. https://doi.org/10.1038/nchembio.2077

Park, J. O., Tanner, L. B., Wei, M. H., Khana, D. B., Jacobson, T. B., Zhang, Z., Rubin, S. A., Li, S. H. J., Higgins, M. B., Stevenson, D. M., Amador-Noguez, D., & Rabinowitz, J. D. (2019). Near-equilibrium glycolysis supports metabolic homeostasis and energy yield. *Nature Chemical Biology*. https://doi.org/10.1038/s41589-019-0364-9

Paulo, J. A., O'Connell, J. D., Everley, R. A., O'Brien, J., Gygi, M. A., & Gygi, S. P. (2016). Quantitative mass spectrometry-based multiplexing compares the abundance of 5000 S. cerevisiae proteins across 10 carbon sources. *Journal of Proteomics*, *148*, 85–93. https://doi.org/10.1016/j.jprot.2016.07.005

Pedruzzi, I., Bürckert, N., Egger, P., & De Virgilio, C. (2000). Saccharomyces cerevisiae Ras/cAMP pathway controls post-diauxic shift element-dependent transcription through the zinc finger

protein Gis1. *The EMBO Journal*, *19*(11), 2569–2579. https://doi.org/10.1093/emboj/19.11.2569

Peeters, K., Van Leemputte, F., Fischer, B., Bonini, B. M., Quezada, H., Tsytlonok, M., Haesen, D., Vanthienen, W., Bernardes, N., Gonzalez-Blas, C. B., Janssens, V., Tompa, P., Versées, W., & Thevelein, J. M. (2017). Fructose-1,6-bisphosphate couples glycolytic flux to activation of Ras. *Nature Communications*, *8*(1). https://doi.org/10.1038/s41467-017-01019-z

Peeters, T., Louwet, W., Geladé, R., Nauwelaers, D., Thevelein, J. M., & Versele, M. (2006). Kelch-repeat proteins interacting with the Gα protein Gpa2 bypass adenylate cyclase for direct regulation of protein kinase A in yeast. *Proceedings of the National Academy of Sciences of the United States of America*, *103*(35), 13034–13039. https://doi.org/10.1073/pnas.0509644103

Portela, P., Howell, S., Moreno, S., & Rossi, S. (2002). In vivo and in vitro phosphorylation of two isoforms of yeast pyruvate kinase by protein kinase A. *Journal of Biological Chemistry*, *277*(34), 30477–30487. https://doi.org/10.1074/jbc.M201094200

Reinke, A., Anderson, S., McCaffery, J. M., Yates, J., Aronova, S., Chu, S., Fairclough, S., Iverson, C., Wedaman, K. P., & Powers, T. (2004). TOR Complex 1 Includes a Novel Component, Tco89p (YPL180w), and Cooperates with Ssd1p to Maintain Cellular Integrity in Saccharomyces cerevisiae. *Journal of Biological Chemistry*, *279*(15), 14752–14762. https://doi.org/10.1074/jbc.M313062200

Rittenhouse, J., Moberly, L., & Marcus, F. (1987). Phosphorylation in vivo of yeast (Saccharomyces cerevisiae) fructose-1,6-bisphosphatase at the cyclic AMP-dependent site. *Journal of Biological Chemistry*, *262*(21), 10114–10119.

Robertson, L. S., & Fink, G. R. (1998). The three yeast A kinases have specific signaling functions in pseudohyphal growth. *Proceedings of the National Academy of Sciences of the United States of America*, *95*(23), 13783–13787. https://doi.org/10.1073/pnas.95.23.13783

Robinson, L. C., Gibbs, J. B., Marshall, M. S., Sigal, I. S., & Tatchell, K. (1987). CDC25: A component of the RAS-adenylate cyclase pathway in Saccharomyces cerevisiae. *Science*, *235*(4793), 1218–1221. https://doi.org/10.1126/science.3547648

Rolland, F., De Winde, J. H., Lemaire, K., Boles, E., Thevelein, J. M., & Winderickx, J. (2000). Glucose-induced cAMP signalling in yeast requires both a G-protein coupled receptor system for extracellular glucose detection and a separable hexose kinase-dependent sensing process. *Molecular Microbiology*, *38*(2), 348–358. https://doi.org/10.1046/j.1365-2958.2000.02125.x

Romers, J., Thieme, S., Münzner, U., & Krantz, M. (2020). A scalable method for parameter-free simulation and validation of mechanistic cellular signal transduction network models. *Npj Systems Biology and Applications*, *6*(1). https://doi.org/10.1038/s41540-019-0120-5

Salminen, A., & Kaarniranta, K. (2012). AMP-activated protein kinase (AMPK) controls the aging process via an integrated signaling network. In *Ageing Research Reviews* (Vol. 11, Issue 2, pp. 230–241). Elsevier. https://doi.org/10.1016/j.arr.2011.12.005

Sánchez, B. J., Zhang, C., Nilsson, A., Lahtvee, P., Kerkhoven, E. J., & Nielsen, J. (2017). Improving the phenotype predictions of a yeast genome□scale metabolic model by incorporating

enzymatic constraints. *Molecular Systems Biology*, *13*(8), 935. https://doi.org/10.15252/msb.20167411

Santangelo, G. M. (2006). Glucose Signaling in Saccharomyces cerevisiae. *Microbiology and Molecular Biology Reviews*, *70*(1), 253–282. https://doi.org/10.1128/mmbr.70.1.253-282.2006

Sanz, P., Alms, G. R., Haystead, T. A. J., & Carlson, M. (2000). Regulatory Interactions between the Reg1-Glc7 Protein Phosphatase and the Snf1 Protein Kinase. *Molecular and Cellular Biology*, *20*(4), 1321–1328. https://doi.org/10.1128/mcb.20.4.1321-1328.2000

Sass, P., Field, J., Nikawa, J., Toda, T., & Wigler, M. (1986). Cloning and characterization of the high-affinity cAMP phosphodiesterase of Saccharomyces cerevisiae. *Proceedings of the National Academy of Sciences of the United States of America*, *83*(24), 9303–9307. https://doi.org/10.1073/pnas.83.24.9303

Schepers, W., Van Zeebroeck, G., Pinkse, M., Verhaert, P., & Thevelein, J. M. (2012). In vivo phosphorylation of Ser21 and Ser83 during nutrient-induced activation of the yeast protein kinase A (PKA) target trehalase. *Journal of Biological Chemistry*, *287*(53), 44130–44142. https://doi.org/10.1074/jbc.M112.421503

Schuetz, R., Kuepfer, L., & Sauer, U. (2007). Systematic evaluation of objective functions for predicting intracellular fluxes in Escherichia coli. *Molecular Systems Biology*. https://doi.org/10.1038/msb4100162

Schüller, H. J. (2003). Transcriptional control of nonfermentative metabolism in the yeast Saccharomyces cerevisiae. *Current Genetics*, *43*(3), 139–160. https://doi.org/10.1007/s00294-003-0381-8

Shashkova, S., Welkenhuysen, N., & Hohmann, S. (2015). Molecular communication: crosstalk between the Snf1 and other signaling pathways. *FEMS Yeast Research*, *15*. https://doi.org/10.1093/femsyr/fov026

Shlomi, T., Eisenberg, Y., Sharan, R., & Ruppin, E. (2007). A genome-scale computational study of the interplay between transcriptional regulation and metabolism. *Molecular Systems Biology*, *3*, 101. https://doi.org/10.1038/msb4100141

Siegle, L., Schwab, J. D., Kühlwein, S. D., Lausser, L., Tümpel, S., Pfister, A. S., Kühl, M., & Kestler, H. A. (2018). A Boolean network of the crosstalk between IGF and Wnt signaling in aging satellite cells. *PLoS ONE*, *13*(3). https://doi.org/10.1371/journal.pone.0195126

Smith, J. J., Miller, L. R., Kreisberg, R., Vazquez, L., Wan, Y., & Aitchison, J. D. (2011). Environment-responsive transcription factors bind subtelomeric elements and regulate gene silencing. *Molecular Systems Biology*, *7*, 455. https://doi.org/10.1038/msb.2010.110

Soontorngun, N., Baramee, S., Tangsombatvichit, C., Thepnok, P., Cheevadhanarak, S., Robert, F., & Turcotte, B. (2012). Genome-wide location analysis reveals an important overlap between the targets of the yeast transcriptional regulators Rds2 and Adr1. *Biochemical and Biophysical Research Communications*, *423*(4), 632–637. https://doi.org/10.1016/j.bbrc.2012.05.151

Steinberg, G. R., & Kemp, B. E. (2009). AMPK in Health and Disease. *Physiological Reviews*, *89*(3),

970 1025–1078. https://doi.org/10.1152/physrev.00011.2008

971 Sulaimanov, N., Klose, M., Busch, H., & Boerries, M. (2017). Understanding the mTOR signaling
972 pathway via mathematical modeling. In *Wiley Interdisciplinary Reviews: Systems Biology and*
973 *Medicine* (Vol. 9, Issue 4). Wiley-Blackwell. https://doi.org/10.1002/wsbm.1379

974 Sutherland, C. M., Hawley, S. A., McCartney, R. R., Leech, A., Stark, M. J. R., Schmidt, M. C., &
975 Hardie, D. G. (2003). Elm1p is one of three upstream kinases for the Saccharomyces cerevisiae
976 SNF1 complex. *Current Biology : CB*, *13*(15), 1299–1305. https://doi.org/10.1016/s0960-
977 9822(03)00459-7

978 Swinnen, E., Wanke, V., Roosen, J., Smets, B., Dubouloz, F., Pedruzzi, I., Cameroni, E., De Virgilio,
979 C., & Winderickx, J. (2006). Rim15 and the crossroads of nutrient signalling pathways in
980 Saccharomyces cerevisiae. In *Cell Division* (Vol. 1, p. 3). BioMed Central.
981 https://doi.org/10.1186/1747-1028-1-3

982 Tanaka, K, Matsumoto, K., & Toh-E, A. (1989). IRA1, an inhibitory regulator of the RAS-cyclic
983 AMP pathway in Saccharomyces cerevisiae. *Molecular and Cellular Biology*, *9*(2), 757–768.
984 https://doi.org/10.1128/mcb.9.2.757

985 Tanaka, K, Nakafuku, M., Tamanoi, F., Kaziro, Y., Matsumoto, K., & Toh-e, A. (1990). IRA2, a
986 second gene of Saccharomyces cerevisiae that encodes a protein with a domain homologous to
987 mammalian ras GTPase-activating protein. *Molecular and Cellular Biology*, *10*(8), 4303–4313.
988 https://doi.org/10.1128/mcb.10.8.4303

989 Tanaka, Kazuma, Nakafuku, M., Satoh, T., Marshall, M. S., Gibbs, J. B., Matsumoto, K., Kaziro, Y.,
990 & Toh-e, A. (1990). S. cerevisiae genes IRA1 and IRA2 encode proteins that may be
991 functionally equivalent to mammalian ras GTPase activating protein. *Cell*, *60*(5), 803–807.
992 https://doi.org/10.1016/0092-8674(90)90094-U

993 Tanner, L. B., Goglia, A. G., Wei, M. H., Sehgal, T., Parsons, L. R., Park, J. O., White, E., Toettcher,
994 J. E., & Rabinowitz, J. D. (2018). Four Key Steps Control Glycolytic Flux in Mammalian Cells.
995 *Cell Systems*. https://doi.org/10.1016/j.cels.2018.06.003

996 Thompson-Jaeger, S., Francois, J., Gaughran, J. P., & Tatchell, K. (1991). Deletion of SNF1 affects
997 the nutrient response of yeast and resembles mutations which activate the adenylate cyclase
998 pathway. *Genetics*, *129*(3), 697–706.

999 Toda, T, Cameron, S., Sass, P., Zoller, M., Scott, J. D., McMullen, B., Hurwitz, M., Krebs, E. G., &
1000 Wigler, M. (1987). Cloning and characterization of BCY1, a locus encoding a regulatory
1001 subunit of the cyclic AMP-dependent protein kinase in Saccharomyces cerevisiae. *Molecular*
1002 *and Cellular Biology*, *7*(4), 1371–1377. https://doi.org/10.1128/mcb.7.4.1371

1003 Toda, Takashi, Cameron, S., Sass, P., Zoller, M., & Wigler, M. (1987). Three different genes in S.
1004 cerevisiae encode the catalytic subunits of the cAMP-dependent protein kinase. *Cell*, *50*(2),
1005 277–287. https://doi.org/10.1016/0092-8674(87)90223-6

1006 Toda, Takashi, Uno, I., Ishikawa, T., Powers, S., Kataoka, T., Broek, D., Cameron, S., Broach, J.,
1007 Matsumoto, K., & Wigler, M. (1985). In yeast, RAS proteins are controlling elements of
1008 adenylate cyclase. *Cell*, *40*(1), 27–36. https://doi.org/10.1016/0092-8674(85)90305-8

Turcotte, B., Liang, X. B., Robert, F., & Soontorngun, N. (2010). Transcriptional regulation of nonfermentable carbon utilization in budding yeast. In *FEMS Yeast Research* (Vol. 10, Issue 1, pp. 2–13). PMC Canada manuscript submission. https://doi.org/10.1111/j.1567-1364.2009.00555.x

Urban, J., Soulard, A., Huber, A., Lippman, S., Mukhopadhyay, D., Deloche, O., Wanke, V., Anrather, D., Ammerer, G., Riezman, H., Broach, J. R., De Virgilio, C., Hall, M. N., & Loewith, R. (2007). Sch9 Is a Major Target of TORC1 in Saccharomyces cerevisiae. *Molecular Cell*, *26*(5), 663–674. https://doi.org/10.1016/j.molcel.2007.04.020

Van Hoek, P., Van Dijken, J. P., & Pronk, J. T. (1998). Effect of specific growth rate on fermentative capacity of baker's yeast. *Applied and Environmental Microbiology*, *64*(11), 4226–4233. https://doi.org/10.1128/AEM.64.11.4226-4233.1998

Varma, A., & Palsson, B. O. (1994). Metabolic flux balancing: Basic concepts, scientific and practical use. *Bio/Technology*. https://doi.org/10.1038/nbt1094-994

Vega, M., Riera, A., Fernández-Cid, A., Herrero, P., & Moreno, F. (2016). Hexokinase 2 Is an intracellular glucose sensor of yeast cells that maintains the structure and activity of mig1 protein repressor complex. *Journal of Biological Chemistry*. https://doi.org/10.1074/jbc.M115.711408

Walpole, J., Papin, J. A., & Peirce, S. M. (2013). Multiscale Computational Models of Complex Biological Systems. *Annual Review of Biomedical Engineering*, *15*(1), 137–154. https://doi.org/10.1146/annurev-bioeng-071811-150104

Wang, M., Herrmann, C. J., Simonovic, M., Szklarczyk, D., & von Mering, C. (2015a). Version 4.0 of PaxDb: Protein abundance data, integrated across model organisms, tissues, and cell-lines. *Proteomics*. https://doi.org/10.1002/pmic.201400441

Wang, M., Herrmann, C. J., Simonovic, M., Szklarczyk, D., & von Mering, C. (2015b). Version 4.0 of PaxDb: Protein abundance data, integrated across model organisms, tissues, and cell-lines. *Proteomics*, *15*(18), 3163–3168. https://doi.org/10.1002/pmic.201400441

Wang, Y. P., & Lei, Q. Y. (2018). Metabolite sensing and signaling in cell metabolism. In *Signal Transduction and Targeted Therapy* (Vol. 3, Issue 1, pp. 1–9). Springer Nature. https://doi.org/10.1038/s41392-018-0024-7

Wanke, V., Cameroni, E., Uotila, A., Piccolis, M., Urban, J., Loewith, R., & De Virgilio, C. (2008). Caffeine extends yeast lifespan by targeting TORC1. *Molecular Microbiology*, *69*(1), 277–285. https://doi.org/10.1111/j.1365-2958.2008.06292.x

Welkenhuysen, N., Borgqvist, J., Backman, M., Bendrioua, L., Goksör, M., Adiels, C. B., Cvijovic, M., & Hohmann, S. (2017). Single-cell study links metabolism with nutrient signaling and reveals sources of variability. *BMC Systems Biology*, *11*(1). https://doi.org/10.1186/s12918-017-0435-z

Welkenhuysen, N., Schnitzer, B., Österberg, L., & Cvijovic, M. (2019). Robustness of nutrient signaling is maintained by interconnectivity between signal transduction pathways. *Frontiers in Physiology*, *10*(JAN), 1964. https://doi.org/10.3389/fphys.2018.01964

Westholm, J. O., Nordberg, N., Murén, E., Ameur, A., Komorowski, J., & Ronne, H. (2008). Combinatorial control of gene expression by the three yeast repressors Mig1, Mig2 and Mig3. *BMC Genomics*, *9*(SUPPL. 2), 601. https://doi.org/10.1186/1471-2164-9-601

Wierman, M. B., Maqani, N., Strickler, E., Li, M., & Smith, J. S. (2017). Caloric Restriction Extends Yeast Chronological Life Span by Optimizing the Snf1 (AMPK) Signaling Pathway. *Molecular and Cellular Biology*, *37*(13). https://doi.org/10.1128/mcb.00562-16

Wiśniewski, J. R., & Rakus, D. (2014). Multi-enzyme digestion FASP and the 'Total Protein Approach'-based absolute quantification of the Escherichia coli proteome. *Journal of Proteomics*. https://doi.org/10.1016/j.jprot.2014.07.012

Woods, A., Munday, M. R., Scott, J., Yang, X., Carlson, M., & Carling, D. (1994). Yeast SNF1 is functionally related to mammalian AMP-activated protein kinase and regulates acetyl-CoA carboxylase in vivo. *Journal of Biological Chemistry*, *269*(30), 19509–19515.

Yan, G., Shen, X., & Jiang, Y. (2006). Rapamycin activates Tap42-associated phosphatases by abrogating their association with Tor complex 1. *EMBO Journal*, *25*(15), 3546–3555. https://doi.org/10.1038/sj.emboj.7601239

Yilmaz, L. S., & Walhout, A. J. (2017). Metabolic network modeling with model organisms. In *Current Opinion in Chemical Biology* (Vol. 36, pp. 32–39). Elsevier Ltd. https://doi.org/10.1016/j.cbpa.2016.12.025

Metabolic layer

Metabolic network

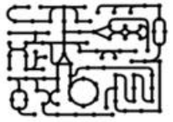

Gecko

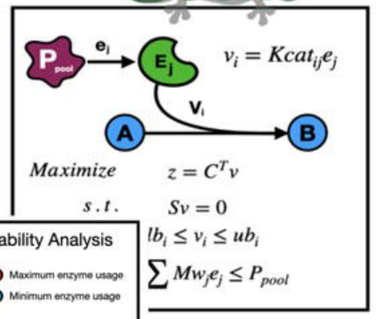

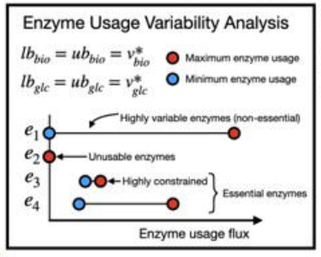

Enzyme-constrained Model

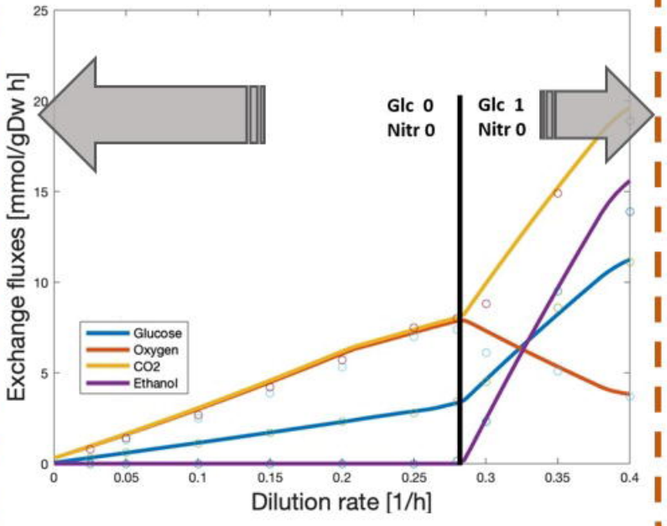

Signaling layer

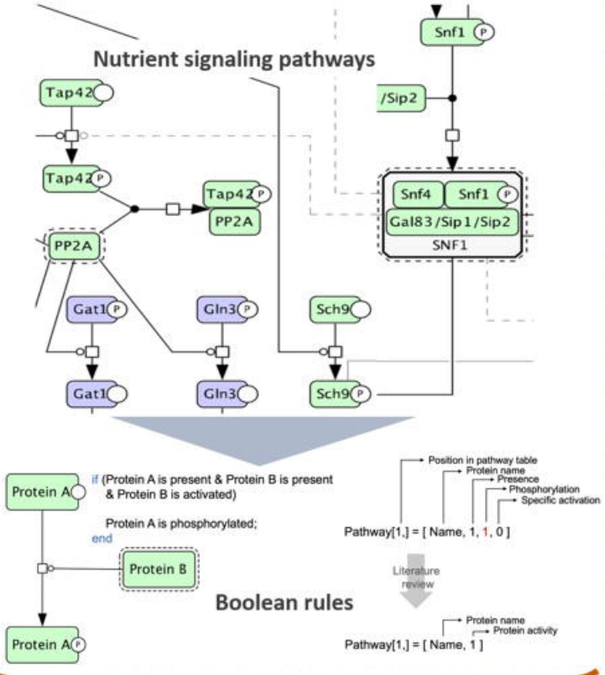

Transcriptional layer

TF	positive	negative
Gis1p	ADH1,TDH1,COX5B,PGK1,CIT1,ENO1,PDC1,FBP1,ERR1,ERR2,PCK1,ZWF1,PDX1,PDC5,PDC6,ICL1,MLS1,TKL2,GPP1,ERR3,CIT3,YJL045W,ALD2,GND2,TIM11,NDE2	QCR7,COX6,ATP2,COX8,HXK2,CYT1,COX9,COR1,RIP1,QCR8,ATP5,COX7,MDH1,KGD1,ATP15,SDH2,ATP7,NDI1,COX13,QCR10,ATP3,NDE1,GPD2,SOL4,ATP19,GPD1,SDH1,COX12,ATP17,ATP16,ATP20,ATP14
Msn2	TDH1,COX5B,CIT1,GAL10,HXK1,ATP4,PDC1,GAL7,ERR1,ERR2,COX7,PDX1,MDH1,GLK1,COX11,ATP15,SDH2,QCR9,ATP7,NDI1,TKL2,SDH3,PGM2,COX23,GPP2,ERR3,CIT3,ALD4,ALD2,PYK2,LSC2,GPD1,HFD1,COX20,ATP20	TDH2,CDC19,PGK1,ENO1,GPM1,COX4,HXK2,COX9,COR1,PGI1,FBA1,PFK1,PFK2,PGM1,GND1,NDE1,ACS2,SOL4,FAP7
	COX5B,HXK1,PDC1,COX7,PDX1,MDH1,GLK1,C	

Yeastract

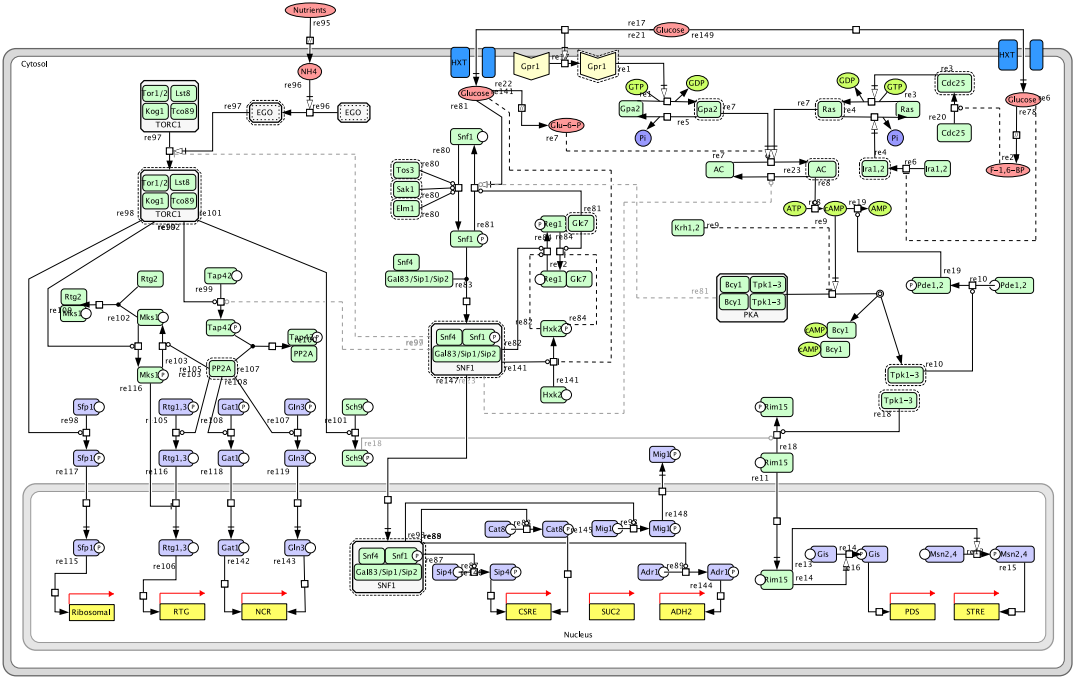
Nutrients
re95
Cytosol
NH4
re96
Tor1/2
Lst8
Kog1
Tco89
TORC1
re97
EGO
EGO
re96
re97
Tor1/2
Lst8
Kog1
Tco89
TORC1
re98
re101
re102
Rtg2
Mks1
Tap42
re99
Mks1
Tap42
PP2A
PP2A
re103
re104
re107
re108
Mks1
re116
Sfp1
Rtg1,3
Gat1
Gln3
Sch9
re98
re105
re107
re101
re18
Sfp1
Rtg1,3
Gat1
Gln3
Sch9
re117
re116
re118
re119
Sfp1
Rtg1,3
Gat1
Gln3
re115
re106
re142
re143
Ribosomal
RTG
NCR
HXT
re17
re21
Glucose
re149
Gpr1
re2
Gpr1
re1
re22
Glucose
re141
re81
Glu-6-P
re7
GTP
GDP
Gpa2
re3
Gpa2
re7
re5
Pi
Snf1
re80
Tos3
Sak1
Elm1
re80
Snf1
re81
Reg1
Glc7
re83
Reg1
Glc7
re82
Snf4
Gal83/Sip1/Sip2
re85
Hxk2
re84
Hxk2
Snf4
Snf1
Gal83/Sip1/Sip2
SNF1
re82
re141
re147
re93
re141
Hxk2
HXT
Glucose
re6
re74
Ras
re4
Ras
GTP
GDP
re3
Cdc25
Cdc25
re20
re7
Pi
re4
AC
re23
AC
re8
Ira1,2
re6
Ira1,2
re24
F-1,6-BP
ATP
re8
AMP
re10
AMP
re9
Krh1,2
re9
Bcy1
Tpk1-3
Bcy1
Tpk1-3
PKA
re19
Pde1,2
re10
Pde1,2
AMP
Bcy1
AMP
Bcy1
Tpk1-3
re10
Tpk1-3
re18
Xim15
re18
Xim15
re11
Mig1
Mig1
re148
Cat8
re88
Cat8
re145
Mig1
re89
Mig1
Snf4
Snf1
Gal83/Sip1/Sip2
SNF1
re87
Sip4
re86
Sip4
Adr1
re88
Adr1
re144
Gis
re14
Gis
re13
re16
Xim15
re14
Msn2,4
re15
Msn2,4
CSRE
SUC2
ADH2
PDS
STRE
Nucleus

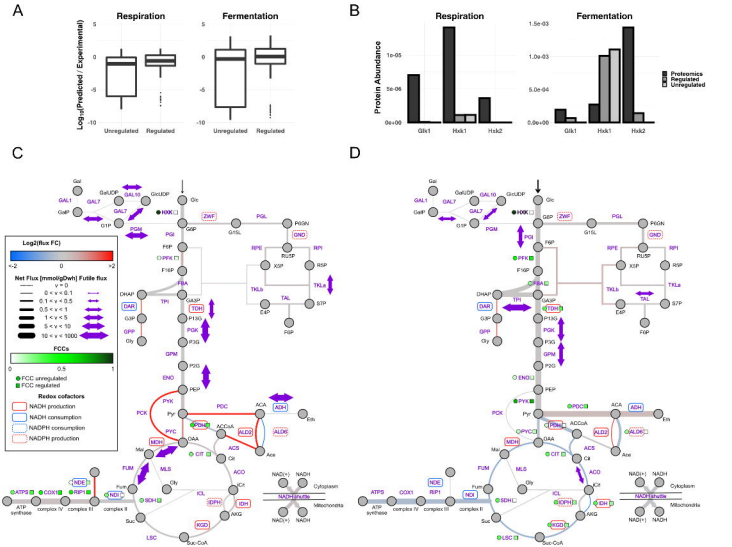
A
Respiration
Fermentation
Log2(Predicted / Experimental)
Unregulated
Regulated
B
Respiration
Fermentation
Protein Abundance
Glk1
Hxk1
Hxk2
Proteomics
Regulated
Unregulated
C
D
Log2(flux FC)
Net Flux [mmol/gDwh] Futile flux
FCCs
FCC unregulated
FCC regulated
Redox cofactors
NADH production
NADH consumption
NADPH consumption
NADPH production
Cytoplasm
Mitochondria
ATP synthase
complex IV
complex III
complex II